Inorg. Chem. **2006**, *45*, 868–876

Five New Manganese–μ-Azido 2D Compounds Synthesized in Aqueous Hydrazoic Acid from Pyrazine Derivatives

Brigitte Bitschnau,[†] Andreas Egger,[†] Albert Escuer,[‡] Franz A. Mautner,[†] Beate Sodin,[†] and Ramon Vicente*[,‡]

Institut für Physikalische and Theoretische Chemie, Technische Universität Graz, A-8010 Graz, Austria, and Departament de Química Inorgànica, Universitat de Barcelona, Diagonal 647, 08028 Barcelona, Spain

Received July 27, 2005

The syntheses, structural characterization, and magnetic behavior of five new 2D manganese(II) complexes with empirical formulas $[Mn(N_3)_2(2,6\text{-DiMepyz})(H_2O)]_n$ (**1**), $[Mn(N_3)_2(Etpyz)(H_2O)]_n$ (**2**), $[Mn(N_3)_2(H_2O)_2]_n(2,3\text{-DiMepyz})_n$ (**3**), $[Mn(N_3)_2(Clpyz)_2]_n$ (**4**), and $[Mn(N_3)_2(Ipyz)_2]_n$ (**5**) (pyz = pyrazine (1,4-diazine)) are reported. **1** crystallizes in the monoclinic system, space group $P2_1/c$, with unit cell parameters $a = 7.513(4)$ Å, $b = 17.438(7)$ Å, $c = 8.404(4)$ Å, $\beta = 94.53(4)°$, and $Z = 4$. **2** crystallizes in the triclinic system, space group $P\bar{1}$, with unit cell parameters $a = 7.386(2)$ Å, $b = 8.434(2)$ Å, $c = 9.442(3)$ Å, $\alpha = 71.82(2)°$, $\beta = 72.08(2)°$, $\gamma = 88.54(2)°$, and $Z = 2$. **3** crystallizes in the monoclinic system, space group $C2/c$, with unit cell parameters $a = 20.438(7)$ Å, $b = 7.711(2)$ Å, $c = 7.457(2)$ Å, $\beta = 93.76(3)°$, and $Z = 4$. **4** crystallizes in the orthorhombic system, space group *Pbca*, with unit cell parameters $a = 8.600(2)$ Å, $b = 13.440(4)$ Å, $c = 24.083(7)$ Å, and $Z = 8$. **5** crystallizes in the orthorhombic system, space group *Pbca*, with unit cell parameters $a = 8.521(2)$ Å, $b = 13.787(3)$ Å, $c = 26.237(5)$ Å, and $Z = 8$. The compounds **1**–**5** have only azido bridging ligands. In **1**–**3** each manganese atom is linked to the four nearest neighbors by only end-to-end azido bridges, forming square layers. **4** and **5** show alternating end-to-end and end-on azido bridges between manganese atoms. The magnetic properties of **1**–**5** are reported. At high temperatures the plots of χ_M or $\chi_M T$ vs T for the **1**–**3** compounds can be fitted as homogeneous 2D systems with $J = -4.9$, -4.4, and -3.9 cm^{-1} for **1**–**3**, respectively. For **1**, **3**, and **5** magnetic ordering and spontaneous magnetizations is achieved below $T_c = 35$, 29, and 22 K, respectively, whereas **2** and **4** do not show spontaneous magnetization up to 2 K.

Introduction

Compounds with formula $[Mn(N_3)_2(L)_2]$, L usually R-pyridine monodentate ligands or $(L)_2$ one bidentate aromatic N-donor ligand, show all the range of dimensionalities: from molecular to 3D systems.[1−45] Furthermore, the ability of the azido bridging ligand to coordinate in $\mu_{1,3}$ (end-to-end, EE) or $\mu_{1,1}$ (end-on, EO) modes, which can be present simultaneously in the same $[Mn(N_3)_2(L)_2]$ compound, generates a

* To whom correspondence should be addressed. E-mail: ramon.vicente@qi.ub.es. Fax: ++34934907725.
[†] Technische Universität Graz.
[‡] Universitat de Barcelona.

(1) Ribas, J.; Escuer, A.; Monfort, M.; Vicente, R.; Cortés, R.; Lezama, L.; Rojo, T. *Coord. Chem. Rev.* **1999**, *193*−*195*, 1027.
(2) Escuer, A.; Vicente, R.; Goher, M. A. S.; Mautner, F. A. *Inorg. Chem.* **1995**, *34*, 5707.
(3) Escuer, A.; Vicente, R.; Goher, M. A. S.; Mautner, F. A. *J. Chem. Soc., Dalton Trans.* **1997**, 4431.
(4) Goher, M. A. S.; Abu-Youssef, M. A. M.; Mautner, F. A.; Vicente, R.; Escuer, A. *Eur. J. Inorg. Chem.* **2000**, 1819.
(5) Gao, E.-Q.; Wang, Z.-M.; Yan, C.-H. *Chem. Commun.* **2003**, 1748.
(6) Escuer, A.; Vicente, R.; Goher, M. A. S.; Mautner, F. A. *Inorg. Chem.* **2000**, *39*, 4688.
(7) Escuer, A.; Vicente, R.; Goher, M. A. S.; Mautner, F. A. *Inorg. Chem.* **1996**, *35*, 6386.
(8) Escuer, A.; Vicente, R.; Goher, M. A. S.; Mautner, F. A. *Inorg. Chem.* **1997**, *36*, 3440.
(9) Goher, M. A. S.; Al-Salem, N. A.; Mautner, F. A. *J. Coord. Chem.* **1998**, *44*, 119.
(10) Shen, Z.; Zuo, J.-L.; Yu, Z.; Zhang, Y.; Bai, J.-F.; Che, C.-M.; Fun, H.-K.; Vittal, J. J.; You, X.-Z. *J. Chem. Soc., Dalton Trans.* **1999**, 3393.
(11) Escuer, A.; Mautner, F. A.; Goher, M. A. S.; Abu-Youssef, M. A. M.; Vicente, R. *Chem. Commun.* **2005**, 605.
(12) Abu-Youssef, M. A. M.; Escuer, A.; Goher, M. A. S.; Mautner, F. A.; Vicente, R. *Eur. J. Inorg. Chem.* **1999**, 687.
(13) Abu-Youssef, M. A. M.; Escuer, A.; Gatteschi, D.; Goher, M. A. S.; Mautner, F. A.; Vicente, R. *Inorg. Chem.* **1999**, *38*, 5716.
(14) De Munno, G.; Armentano, D.; Poerio, T.; Julve, M.; Real, J. A. *J. Chem. Soc., Dalton Trans.* **1999**, 1813.

10.1021/ic051258z CCC: $33.50
Published on Web 12/23/2005

great number of topologies in the high dimensional compounds. Taking into account that the EE coordination mode typically promotes antiferromagnetic, AF, interactions and the EO coordination mode promotes ferromagnetic, F, interactions, the great diversity of dimensionalities and topologies found in the $[Mn(N_3)_2(L)_2]$ compounds has as consequence a great diversity in their magnetic behavior. Focusing our attention in the two-dimensional neutral manganese−azido complexes with only azido as bridging ligands and general formula $[Mn(N_3)_2(L)_2]$, we have characterized four topologies to date which can be described as the following: square layers with only EE single azido bridges[2−5] (see Chart 1, **1a**); dinuclear $[Mn_2(\mu_{1,3-}N_3)_2]^{2+}$ units connected in the same plane to four similar entities through end-to-end azido bridges[6] (Chart 1, **1b**); dinuclear $[Mn_2(\mu_{1,1-}N_3)_2]^{2+}$ units connected in the same plane to four similar entities through end-to-end azido bridges[6−9] (Chart 1, **1c**); and the recently published 2D topologic ferrimagnet in which the planes can be described as Mn−$(\mu_{1,1}$-$N_3)_2$−Mn dinuclear subunits linked by means of end-to-end azido bridges and an intermediate Mn(II) center[11] (Chart 1, **1d**). From the magnetic point of view, between the two-dimensional neutral manganese−azido complexes with **1a**,**c** topologies can be found several examples of molecule-based magnets due to the spin-canting phenomenon.[1] The design of molecule-based magnets has been of considerable interest in recent years, and in this context, here we present a new synthetic strategy to prepare new examples of two-dimensional neutral manganese−azido complexes with only azido as bridging ligands from the reaction of manganese(II) nitrate with pyrazine derivatives and diluted hydrazoic acid in aqueous media. The new compounds are $[Mn(N_3)_2$-(2,6-DiMepyz)$(H_2O)]_n$ (**1**), $[Mn(N_3)_2(Etpyz)(H_2O)]_n$ (**2**), $[Mn$-$(N_3)_2(H_2O)_2]_n(2,3\text{-DiMepyz})_n$ (**3**), $[Mn(N_3)_2(Clpyz)_2]_n$ (**4**), and $[Mn(N_3)_2(Ipyz)_2]_n$ (**5**) (pyz = pyrazine (1,4-diazine)). The 2D compounds **1**−**3** show the square layers topology **1a** but with the novelty to incorporate water as axial ligand. In the case of **1** and **2** the water axial ligand alternates with the pyrazine derivative, but in the case of **3**, water is the only axial ligand and the 2,3-DiMepyz ligand remains uncoordinated. The compounds **4** and **5** show **1c** topology with pyrazine derivatives as axial ligands. From the magnetic point of view, **1, 3**, and **5** are molecule-based magnets built from spin-canted metal−azido layers below $T_c = 35$, 29, and 22 K, respectively. In the paramagnetic region, the magnetic measurements for **1**−**3** show typical behavior of two-dimensional Heisenberg antiferromagnets with $J = -4.9$, -4.4, and -3.9 cm^{-1}, respectively. The compounds **2** and **4** do not show spontaneous magnetization up to 2 K.

Experimental Section

Starting Materials. Manganese(II) nitrate tetrahydrate, pyrazine derivative ligands, and sodium azide (Aldrich) were used as obtained. Aqueous hydrazoic acid is obtained with a modified Kipp's generator by decomposition of NaN_3 in H_2SO_4/H_2O (1:3, v:v) and subsequent transfer of HN_3 into H_2O with aid of an inert-gas stream.[46]

Caution! Azide compounds and hydrazoic acid (HN_3) are potentially explosive! Only a small amount of material should be prepared, and it should be handled with care.

Spectral and Magnetic Measurements. Infrared spectra (4000−400 cm^{-1}) were recorded from KBr pellets on a Perkin-Elmer 380-B spectrophotometer. Magnetic susceptibility measurements under several magnetic fields in the temperature range 2−300 K and magnetization measurements in the field range of 0−5 T were performed with a Quantum Design MPMS-XL SQUID magnetometer at the Magnetochemistry Service of the University of Barcelona. All measurements were performed on polycrystalline samples. Pascal's constants were used to estimate the diamagnetic correc-

(15) Hong, C. S.; Son, S. K.; Lee, Y. S.; Jun, M. J.; Do, Y. *Inorg. Chem.* **1999**, *38*, 5602.
(16) Liu, C.-M.; Yu, Z.; Xiong, R.-G.; Liu, K.; You, X.-Z. *Inorg. Chem. Commun.* **1999**, *2*, 31.
(17) Manson, J. M. L.; Arif, A. M.; Miller, J. S. *Chem. Commun.* **1999**, 1479.
(18) Mautner, F. A.; Hanna, S.; Cortés, R.; Lezama, L.; Barandika, M. G.; Rojo, T. *Inorg. Chem.* **1999**, *38*, 4647.
(19) Tang, L. F.; Zhang, L.; Li, L. C.; Cheng, P.; Wang, Z. H.; Wang, J. T. *Inorg. Chem.* **1999**, *38*, 6326.
(20) Abu-Youssef, M. A. M.; Escuer, A.; Goher, M. A. S.; Mautner, F. A.; Reis, G. J.; Vicente, R. *Angew. Chem., Int. Ed.* **2000**, *39*, 1624.
(21) Abu-Youssef, M. A. M.; Drillon, M.; Escuer, A.; Goher, M. A. S.; Mautner, F. A.; Vicente, R. *Inorg. Chem.* **2000**, *39*, 5022.
(22) Goher, M. A. S.; Cano, J.; Journaux, Y.; Abu-Youssef, M. A. M.; Mautner, F. A.; Escuer, A.; Vicente, R. *Chem.—Eur. J.* **2000**, *6*, 778.
(23) Han, S.; Manson, J. L.; Kim, J.; Miller, J. S. *Inorg. Chem.* **2000**, *39*, 4182.
(24) Hernandez, M.-L.; Barandika, M. G.; Urtiaga, M. K.; Cortés, R.; Lezama, L.; Arriortua, M. I. *J. Chem. Soc., Dalton Trans.* **2000**, 79.
(25) Shen, H. Y.; Bu, W. M.; Gao, E. Q.; Liao, D. Z.; Jiang, Z.-H.; Yan, S.-P.; Wang, G.-L. *Inorg. Chem.* **2000**, *39*, 396.
(26) Sra, A. K.; Sutter, J.-P.; Guionneau, P.; Chasseau, D.; Yakhmi, J. V.; Kahn, O. *Inorg. Chim. Acta* **2000**, *300*, 778.
(27) Abu-Youssef, M. A. M.; Escuer, A.; Goher, M. A. S.; Mautner, F. A.; Vicente, R. *J. Chem. Soc., Dalton Trans.* **2000**, 413.
(28) Zhang, Z.; Bu, X.-H.; Ma, Z.-H.; Bu, W. M.; Tang, Y.; Zhao, Q.-H. *Polyhedron* **2000**, *19*, 1559.
(29) Chen, H.-J.; Mao, Z.-W.; Gao, S.; Chen, X.-M. *Chem. Commun.* **2001**, 2320.
(30) Ma, B.-Q.; Sun, H.-L.; Gao, S.; Su, G. *Chem. Mater.* **2001**, *13*, 1946.
(31) Martín, S.; Barandika, M. G.; Lezama, L.; Pizarro, J. L.; Serna, Z. S.; Ruiz de Larramendi, J. I.; Arriortua, M. I.; Rojo, T.; Cortés, R. *Inorg. Chem.* **2001**, *40*, 4109.
(32) Papaefstathiou, G.; Escuer, A.; Raptopoulou, C. P.; Terzis, A.; Perlepes, S. P.; Vicente, R. *Eur. J. Inorg. Chem.* **2001**, 1567.
(33) Villanueva, M.; Mesa, J. L.; Urtiaga, M. K.; Cortés, R.; Lezama, L.; Arriortua, M. I.; Rojo, T. *Eur. J. Inorg. Chem.* **2001**, 1581.
(34) Karmakar, T. K.; Chandra, S. K.; Ribas, J.; Mostafa, G.; Lu, T. H.; Ghosh, B. K. *Chem. Commun.* **2002**, 2364.
(35) Gao, E. Q.; Bai, S.-Q.; Wang, C.-F.; Yue, Y.-F.; Yan, C.-H. *Inorg. Chem.* **2003**, *42*, 8456.
(36) Gao, E. Q.; Bai, S.-Q.; Yue, Y.-F.; Wang, Z. M.; Yan, C.-H. *Inorg. Chem.* **2003**, *42*, 3642.
(37) Gao, E. Q.; Bai, J.-F.; Wang, Z. M.; Yan, C.-H. *J. Am. Chem. Soc.* **2003**, *125*, 4984.
(38) Gao, E. Q.; Yue, Y.-F.; Bai, S.-Q.; He, Z.; Yan, C.-H. *J. Am. Chem. Soc.* **2004**, *126*, 1419.
(39) Liu, C.-M.; Gao, S.; Zhang, D.-Q.; Huang, Y.-H.; Xiong, R.-G.; Liu, Z.-L.; Jiang, F.-C.; Zhu, D.-B. *Angew. Chem., Int. Ed.* **2004**, *43*, 990.
(40) Ray, U.; Jasimuddin, Sk.; Kumar Ghosh, B.; Monfort, M.; Ribas, J.; Mostafa, G.; Lu, T.-H.; Sinha, C. *Eur. J. Inorg. Chem.* **2004**, 250.
(41) Wang, S.-B.; Yang, G.-M.; Liao, D.-Z.; and Li, L.-C. *Inorg. Chem.* **2004**, *43*, 852.
(42) Deoghoria, S.; Bera, S. K.; Moulton, B.; Zaworotko, M. J.; Tuchages, J. P.; Mostafa, G.; Lu, T. H.; Chandra, S. K. *Polyhedron* **2005**, *24*, 343.
(43) Ghosh, A. K.; Ghoshal, D.; Zangrando, E.; Ribas, J.; Chaudhuri, N. R. *Inorg. Chem.* **2005**, *44*, 1786.
(44) Karmakar, T. K.; Ghosh, B. K.; Usman, A.; Fun, H.-K.; Rivière, E.; Mallah, T.; Aromí, G.; Chandra, S. K. *Inorg. Chem.* **2005**, *44*, 2391.
(45) Liu, C.-M.; Gao, S.; Zhang, D.-Q.; Liu, Z.-L.; Zhu, D.-B. *Inorg. Chim. Acta* **2005**, *358*, 834.
(46) Fair, H. D., Walker, R. F., Eds. *Energetic Materials*; Plenum Press: New York, 1977; Vol. I, pp 25−31.

Chart 1

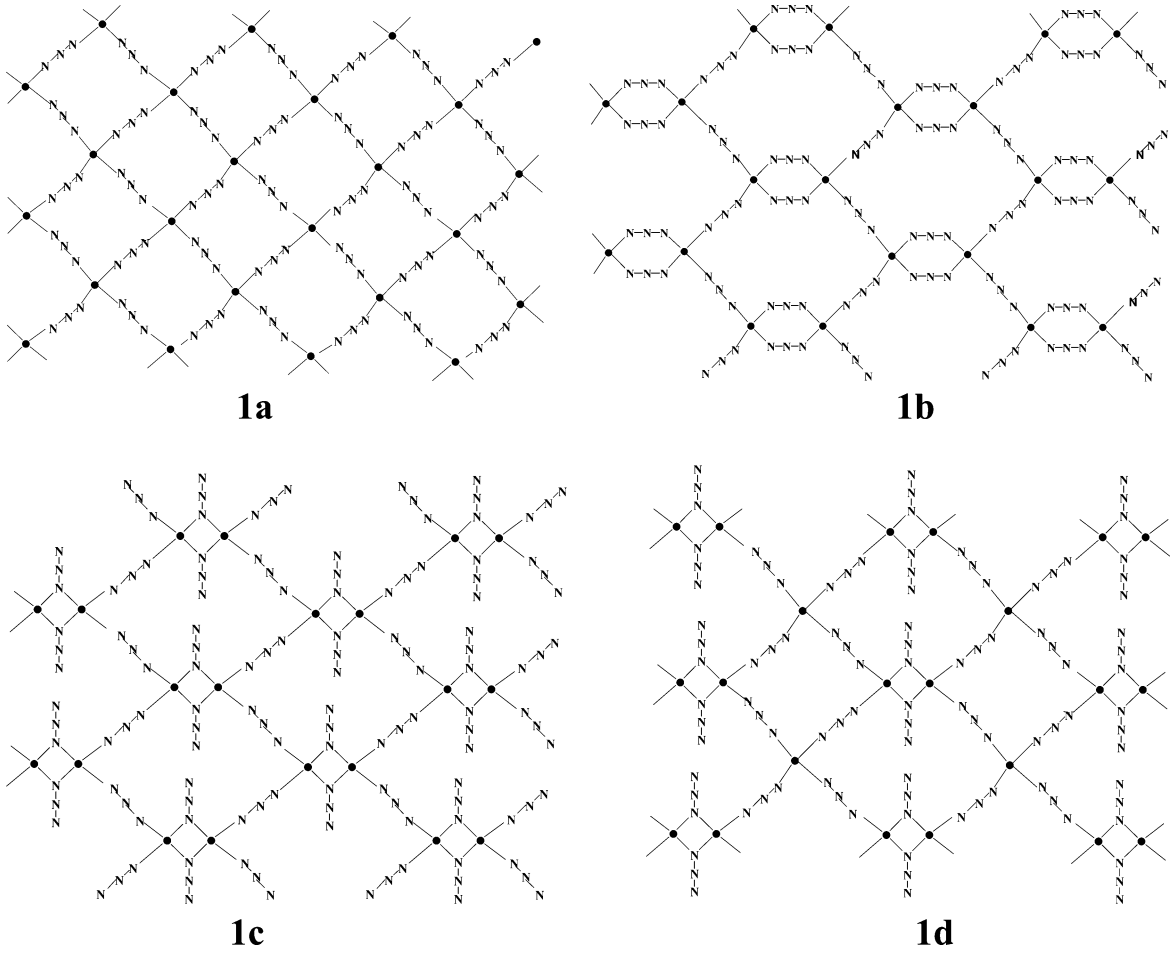

tions, which were subtracted from the experimental susceptibilities to give the corrected molar magnetic susceptibilities.

Synthesis. $[Mn(N_3)_2(2,6\text{-DiMepyz})(H_2O)]_n$ (1). Manganese(II) nitrate tetrahydrate (0.50 g, 2 mmol), sodium azide (0.26 g, 4 mmol), and 2,6-dimethylpyrazine (0.21 g, 2 mmol) were dissolved in the minimum amount of aqueous hydrazoic acid (2 mL). Slow cooling of the solution to 4 °C gave after 2 days compound **1** as transparent green crystals suitable for X-ray determination. (yield approximately 80%). Anal. Found: C, 26.9; H, 3.7; N, 42.1. Calcd for $C_6H_{10}MnN_8O$: C, 27.2; H, 3.8; N, 42.3.

$[Mn(N_3)_2(Etpyz)(H_2O)]_n$ (2). Synthesis was as in the case of **1**. Manganese(II) nitrate tetrahydrate (0.50 g, 2 mmol), sodium azide (0.26 g, 4 mmol), and ethylpyrazine (0.21 g, 2 mmol) were dissolved in aqueous hydrazoic acid[46] (2 mL) at 50 °C. Slow cooling of the clear solution to 4 °C gave after 2 days compound **2** as transparent green crystals (yield approximately 75%). Anal. Found: C, 26.8; H, 3.6; N, 42.0. Calcd for $C_6H_{10}MnN_8O$: C, 27.2; H, 3.8; N, 42.3.

$[Mn(N_3)_2(H_2O)_2]_n(2,3\text{-DiMepyz})_n$ (3). A procedure similar to that for the case of **1** was used. Manganese(II) nitrate tetrahydrate (0.50 g, 2 mmol), sodium azide (0.26 g, 4 mmol), and 2,3-dimethylpyrazine (0.25 g, 2.3 mmol) were dissolved in aqueous hydrazoic acid[46] (1.8 mL). Slow cooling of the solution to 4 °C gave after 3 days compound **3** as transparent colorless crystals (yield approximately 80%). Anal. Found: C, 25.6; H, 4.0; N, 39.2. Calcd for $C_6H_{12}MnN_8O_2$: C, 25.5; H, 4.3; N, 39.6.

$[Mn(N_3)_2(Clpyz)_2]_n$ (4). The same procedure as in the case of **1** was used. Manganese(II) nitrate tetrahydrate (0.50 g, 2 mmol), sodium azide (0.26 g, 4 mmol), and chloropyrazine (0.22 g, 2 mmol) were dissolved in aqueous hydrazoic acid[46] (1.7 mL). Slow cooling of the solution to 4 °C gave after 3 days compound **4** as transparent green crystals (yield approximately 70%). Anal. Found: C, 25.7; H, 1.4; N, 38.3. Calcd for $C_8H_6Cl_2MnN_{10}$: C, 26.1; H, 1.6; N, 38.1.

$[Mn(N_3)_2(Ipyz)_2]_n$ (5). The same procedure as in the case of **1** was used. Manganese(II) nitrate tetrahydrate (0.25 g, 1 mmol), sodium azide (0.13 g, 2 mmol), and iodopyrazine (0.20 g, 1 mmol) were dissolved in aqueous hydrazoic acid[46] (1.0 mL). Slow cooling of the solution to 4 °C gave after 5 days compound **5** as transparent green crystals (yield approximately 60%). Anal. Found: C, 17.6; H, 1.0; N, 25.2. Calcd for $C_8H_6I_2MnN_{10}$: C, 17.4; H, 1.1; N, 25.4.

IR Spectra. In addition to the vibrations of the pyrazine derivate ligands, very strong absorption bands corresponding to the ν_{as} of the azido ligands appeared at 2149 and 2066 cm^{-1} for **1**, at 2155 and 2108 cm^{-1} for **2**, at 2156 and 2105 cm^{-1} for **3**, at 2158 and 2110 cm^{-1} for **4,** and at 2100 and 2064 cm^{-1} for **5**, respectively.

X-ray Crystallography. The X-ray single-crystal data for compounds **1**−**4** were collected on a modified STOE four-circle diffractometer, and data for compound **5**, on a Bruker-AXS SMART APEX CCD diffractometer with graphite-monochromated Mo Kα radiation. The crystallographic data, conditions retained for the intensity data collection, and features of the structure refinements are listed in Table 1. Lorentz−polarization and absorption corrections using the DIFABS[47] computer program were made for **1**−**4** and the SADABS[48] program for **5**. The structures were solved by

(47) Walker, N.; Stuart, D. *Acta Crystallogr*. **1983**, *A39*, 158.
(48) Blessing, R. H. *Acta Crystallogr*. **1995**, *A51*, 33. *SADABS*; Bruker AXS: Madison, WI, 1998.

Table 1. Crystal and Structure Refinement Data for Complexes **1**−**5**

param	**1**	**2**	**3**	**4**	**5**
formula	$C_6H_{10}MnN_8O$	$C_6H_{10}MnN_8O$	$C_6H_{12}MnN_8O_2$	$C_8H_6Cl_2MnN_{10}$	$C_8H_6I_2MnN_{10}$
mol wt	265.16	265.16	283.18	368.07	550.97
cryst syst	monoclinic	triclinic	monoclinic	orthorhombic	orthorhombic
space group	$P2_1/c$	$P\bar{1}$	$C2/c$	*Pbca*	*Pbca*
a/Å	7.513(3)	7.386(2)	20.438(7)	8.600(2)	8.521(2)
b/Å	17.438(7)	8.434(2)	7.711(2)	13.440(4)	13.787(3)
c/Å	8.404(4)	9.442(3)	7.457(2)	24.083(7)	26.237(5)
α/deg	90	71.82(2)	90	90	90
β/deg	94.53(4)	72.08(2)	93.76(3)	90	90
γ/deg	90	88.54(2)	90	90	90
V/Å^3	1097.6(9)	530.1(3)	1172.7(6)	2783.6(13)	3082.2(11)
Z	4	2	4	8	8
T/K	99(2)	100(2)	99(2)	99(2)	100(2)
ρ_{calcd}/g m^{-3}	1.605	1.661	1.604	1.757	2.375
μ/mm^{-1}	1.197	1.239	1.132	1.341	4.872
cryst size/mm^3	0.34 × 0.20 × 0.16	0.26 × 0.26 × 0.14	0.40 × 0.26 × 0.10	0.40 × 0.16 × 0.10	0.22 × 0.18 × 0.12
θ_{max}/deg	25.50	30.00	30.00	25.50	26.38
no. of reflcns collecd	3025	3607	2328	2674	22 224
data	2024	3088	1709	2590	3150
params	157	156	87	190	190
R^a [$I > 2\sigma(I)$]	0.0372	0.0290	0.0353	0.0448	0.0789
R_w^2 (all data)^b	0.1284	0.0770	0.0970	0.1027	0.1871

^{a} $R(F_o) = \sum||F_o| - |F_c||/\sum|F_o|$. ^{b} $R_w(F_o)^2 = \{\sum[w((F_o)^2 - (F_c)^2)^2]/\sum[w((F_o)^4]\}^{1/2}$.

direct methods using the SHELXS-86[49] computer program and refined by full-matrix least-squares methods, using the SHELXL-93[50] program incorporated in the SHELXTL/PC V 5.03.[51] All non-hydrogen atoms were refined anisotropically. The hydrogen atoms were located on calculated positions (C_{ar}−H = 0.930 Å; C_{Me}−H = 0.960 Å; O−H = 0.820 Å), and their isotropic displacement factors were set 1.2 times the value of the equivalent isotropic displacement parameter of the corresponding parent atom. The molecular plots were obtained using the Ortep32 program.[52]

Results and Discussion

Description of the Structures of $[Mn(N_3)_2(2,6\text{-DiMepyz})(H_2O)]_n$ (1), $[Mn(N_3)_2(Etpyz)(H_2O)]_n$ (2), and $[Mn(N_3)_2(H_2O)_2]_n(2,3\text{-DiMepyz})$ (3). The common features of the two-dimensional neutral manganese−azido complexes **1**−**3** are square layers with only EE azido bridges (see Chart 1, **1a**). The structure of **1** is illustrated in Figure 1a. The relevant bond distances and angles are listed in Table 2. There exist two octahedral Mn(II) centers located at inversion centers. The Mn(1) octahedron is formed by nitrogen atoms N(11), N(21), N(11A), and N(21A) of the azide groups and oxygen atoms O(1) and O(1A) of aqua ligands in a trans-arrangement. The *trans*-MnN_6 geometry of Mn(2) is formed by N(13), N(13B), N(23C), and N(23D) of the azide groups and by N(1) and N(1B) of the pyrazine derivative ligands. The Mn−N(azido) bond lengths are in the range 2.188(3)−2.267(3) Å, whereas Mn(1)−O(1) is 2.165(3) and Mn(2)−N(1) is 2.295(3) Å. The azide groups act as end-to-end bridging ligands; the resulting Mn−azido layers are extended along the *ac*-planes of the monoclinic unit cell. The azide

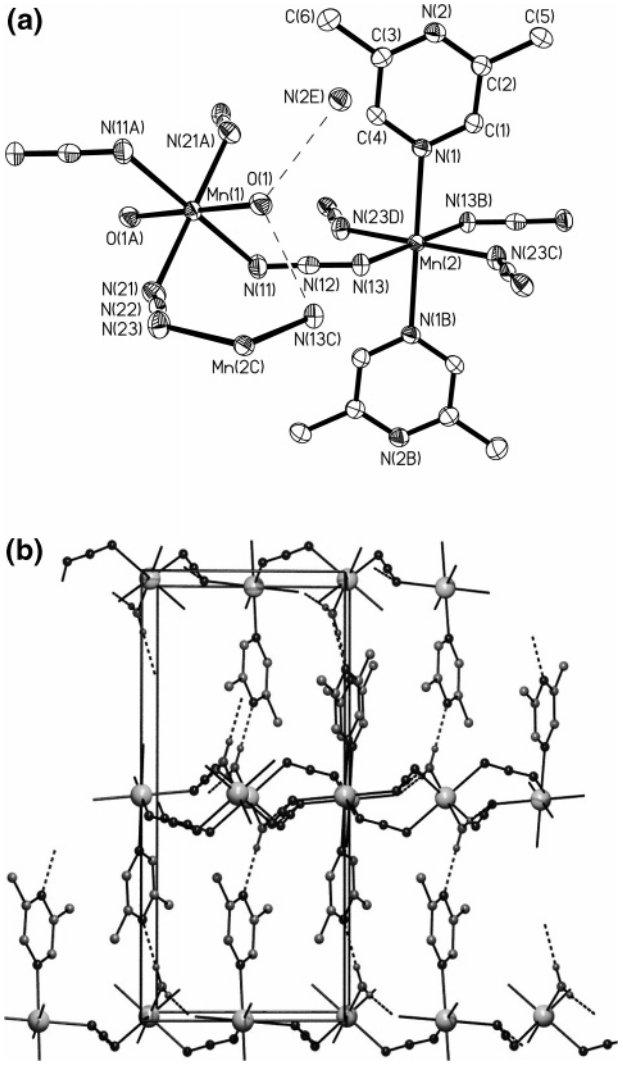

Figure 1. (a) ORTEP drawing of **1** showing the atom-numbering scheme. Ellipsoids are at the 50% probability level. Broken lines indicate hydrogen bonds. Symmetry codes are according Table 2. (b) Packing view of **1**.

(49) Sheldrick, G. M. *SHELXS-86, Program for the Solution of Crystal Structure*; University of Goettingen: Goettingen, Germany, 1986.
(50) Sheldrick, G. M. *SHELXL-93, Program for the Refinement of Crystal Structure*; University of Goettingen: Goettingen, Germany, 1993.
(51) *SHELXTL 5.03 (PC-Version), Program library for the Solution and Molecular Graphics*; Siemens Analytical Instruments Division: Madison, WI, 1995.
(52) Ortep32 for Windows: Farrugia, L. J. *J. Appl. Crystallogr*. **1997**, *30*, 565.

Table 2. Selected Bond Lengths (Å) and Bond Angles (deg) for Complexes **1**−**5**

		Complex **1**[a]			
Mn(1)−N(11A)	2.267(3)	Mn(2)−N(13)	2.216(3)	Mn(1)−N(21)	2.193(3)
Mn(2)−N(23D)	2.188(3)	Mn(1)−O(1)	2.165(3)	Mn(2)−N(1B)	2.295(3)
N(11)−N(12)	1.174(4)	N(12)−N(13)	1.191(4)	N(21)−N(22)	1.178(4)
N(22)−N(23)	1.184(4)	Mn(1)···Mn(2)	5.853(3)	Mn(1)···Mn(2C)	5.411(3)
O(1)···N(2E)	2.818(4)	O(1)···N(13C)	2.908(4)		
N(12)−N(11)−Mn(1)	123.7(2)	N(12)−N(13)−Mn(2)	123.6(2)	N(22)−N(21)−Mn(1)	124.4(2)
N(22)−N(23)−Mn(2C)	132.2(2)	N(11)−N(12)−N(13)	178.8(3)	N(21)−N(22)−N(23)	177.0(3)
		Complex **2**[b]			
Mn(1)−N(11)	2.1979(14)	Mn(2)−N(13)	2.2181(14)	Mn(1)−N(21A)	2.2068(13)
Mn(2)−N(23B)	2.225(2)	Mn(1)−N(1)	2.307(2)	Mn(2)−O(1)	2.1679(12)
N(11)−N(12)	1.174(2)	N(12)−N(13)	1.175(2)	N(21)−N(22)	1.189(2)
N(22)−N(23C)	1.163(2)	Mn(1)···Mn(2)	5.5342(18)	Mn(1)···Mn(2C)	5.6758(18)
N(12)−N(11)−Mn(1)	134.70(11)	N(12)−N(13)−Mn(2)	124.93(11)	N(22)−N(21)−Mn(1)	118.06(10)
N(22C)−N(23)−Mn(2)	130.34(11)	N(11)−N(12)−N(13)	177.4(2)	N(21)−N(22)−N(23C)	178.2(2)
		Complex **3**[c]			
Mn(1)−O(1)	2.1444(12)	Mn(1)−N(11)	2.239(2)	Mn(1)−N(13A)	2.250(2)
N(12)−N(11)	1.184(2)	N(13)−N(12B)	1.167(2)	Mn(1)···Mn(1B)	6.3634(18)
N(11)···O(1B)	2.848(2)	N(1)···O(1B)	2.791(2)		
N(11)−Mn(1)−N(13)	92.19(6)	O(1)−Mn(1)−N(11)	90.65(5)	O(1)−Mn(1)−N(13)	90.74(6)
N(12B)−N(13)−Mn(1)	129.02(11)	N(12)−N(11)−Mn(1)	122.53(11)	N(13)−N(12B)−N(11B)	178.1(2)
		Complex **4**[d]			
Mn(1)···Mn(1A)	3.4214(14)	Mn(1)···Mn(1B)	5.772(2)	Mn(1)−N(23B)	2.185(4)
Mn(1)−N(21)	2.207(4)	Mn(1)−N(11A)	2.211(4)	Mn(1)−N(11)	2.225(4)
Mn(1)−N(3)	2.293(4)	Mn(1)−N(1)	2.309(4)	N(11)−N(12)	1.216(6)
N(12)−N(13)	1.147(6)	N(21)−N(22)	1.184(6)	N(22)−N(23)	1.176(6)
N(3)−Mn(1)−N(1)	175.17(14)	N(12)−N(11)−Mn(1A)	123.1(3)	N(12)−N(11)−Mn(1)	130.3(3)
Mn(1A)−N(11)−Mn(1)	100.9(2)	N(13)−N(12)−N(11)	179.1(5)	N(22)−N(21)−Mn(1)	128.0(3)
N(23)−N(22)−N(21)	177.0(5)	Mn(1)−N(23B)−N(22B)	145.0(4)	N(11A)···N(11)−N(12)	159.6(4)
		Complex **5**[e]			
Mn(1)···Mn(1A)	3.4767(18)	Mn(1)···Mn(1B)	5.845(2)	Mn(1)−N(11A)	2.198(6)
Mn(1)−N(23)	2.201(6)	Mn(1)−N(21)	2.202(6)	Mn(1)−N(11)	2.250(6)
Mn(1)−N(3)	2.296(6)	Mn(1)−N(1)	2.298(6)	N(11)−N(12)	1.224(8)
N(12)−N(13)	1.132(9)	N(21)−N(22)	1.208(8)	N(23)−N(22B)	1.165(8)
N(11A)−Mn(1)−N(23)	166.9(2)	N(3)−Mn(1)−N(1)	175.1(2)	N(23)−Mn(1)−N(21)	100.2(2)
N(11A)−Mn(1)−N(11)	77.2(3)	Mn(1A)−N(11)−Mn(1)	102.8(3)	N(12)−N(11)−Mn(1A)	128.4(5)
N(12)−N(11)−Mn(1)	125.1(5)	N(23C)−N(22)−N(21)	177.5(7)	N(13)−N(12)−N(11)	178.2(8)
N(22)−N(21)−Mn(1)	143.9(5)	N(22B)−N(23)−Mn(1)	136.8(5)	N(11A)···N(11)−N(12)	163.3(9)

[a] Symmetry codes for **1**: (A) $-x+1, -y+1, -z+1$; (B) $-x+2, -y+1, -z$; (C) $-x+2, -y+1, -z+1$; (D) $x, y, z-1$; (E) $x, -y+3/2, z+1/2$. [b] Symmetry codes for **2**: (A) $-x, -y+1, -z+1$; (B) $-x+1, -y, -z+1$; (C) $-x, -y, -z+1$. [c] Symmetry codes for **3**: (A) $-x+1/2, -y+1/2, -z$; (B) $-x+1/2, y+1/2, -z+1/2$; (C) $-x+1, y, -z+3/2$. [d] Symmetry codes for **4**: (A) $-x, -y+2, -z+1$; (B) $x+1/2, -y+3/2, -z+1$; (C) $-x+1/2, y-1/2, z$; (D) $-x-1/2, y+1/2, z$. [e] Symmetry codes for **5**: (A) $-x+1, -y, -z+1$; (B) $x+1/2, -y+1/2, -z+1$; (C) $x-1/2, -y+1/2, -z+1$; (D) $-x+1/2, y-1/2, z$; (E) $-x+3/2, y-1/2, z$.

groups are symmetric with N−N bond lengths in the range from 1.174(4) to 1.191(4) Å and N−N−N angles of 177.0(3) and 178.8(3)°. The Mn−N−N bond angles Mn(1)−N(11)−N(12), Mn(1)−N(21)−N(22), Mn(2)−N(13)−N(12), and Mn(2C)−N(23)−N(22) are 127.7(2), 124.4(2), 123.6(2), and 132.2(2)°, respectively. The Mn(1)···Mn(2) intralayer distances are 5.411(3) and 5.853(3) Å. The Mn(1)−N(11)···N(13)−Mn(2) and Mn(1)−N(21)···N(23)−Mn(2C) torsion angles are −121.7(2) and −59.1(3)°, respectively. The acute angle between the Mn−N(azido) planes [defined by the Mn(1), N(11), N(21), N(11A), N(21A) and Mn(2), N(13), N(13B), N(23C), N(23D) planes, respectively] is 75.04(9)°. Along the *b*-axis the Mn−azido layers are separated by the sheets of 2,6-dimethylpyrazine molecules which act as monodentate ligands via their N(1) donor atoms. A supramolecular 3-D network structure (Figure 1b) is formed by hydrogen bonds of type O−H···N between O(1) of the aqua ligand and uncoordinated N(2) atoms of pyrazine ligands from adjacent layers [O(1)···N(2E) = 2.818(4) Å]. A further intralayer hydrogen bond exists between O(1) and N(13C) with separation of 2.908(4) Å. The shortest interlayer Mn···Mn separation is 9.494(5) Å.

Similar coordination figures as in **1** are observed in the structure of **2** (Figure 2a,b and Table 2). The corresponding MnN_4O_2 and MnN_6 chromophores are located also at inversion centers. The Mn−N(azido) bond lengths are in the range 2.1979(14)−2.225(2) Å, whereas Mn(2)−O(1) is 2.1679(12) and Mn(1)−N(1) is 2.307(2) Å. The azide groups act as end-to-end bridging ligands; the resulting Mn−azido layers are extended along the *ab*-planes of the triclinic unit cell. The azide groups are symmetric with N−N bond lengths in the range from 1.163(2) to 1.189(2) Å and N−N−N angles of 177.4(2) and 178.2(2)°. The Mn−N−N bond angles Mn(1)−N(11)−N(12), Mn(1)−N(21)−N(22), Mn(2)−N(13)−

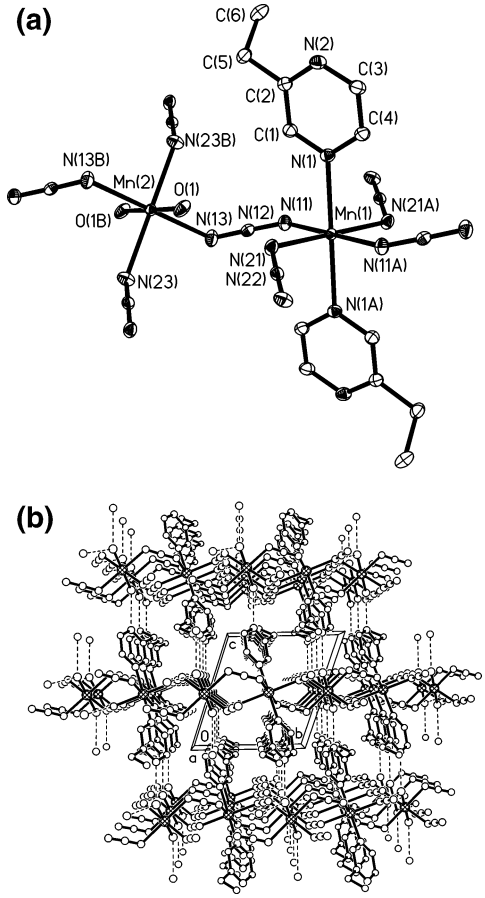

Figure 2. (a) ORTEP drawing of **2** showing the atom-numbering scheme. Ellipsoids are at the 50% probability level. Symmetry codes are according Table 2. (b) Packing view of **2**.

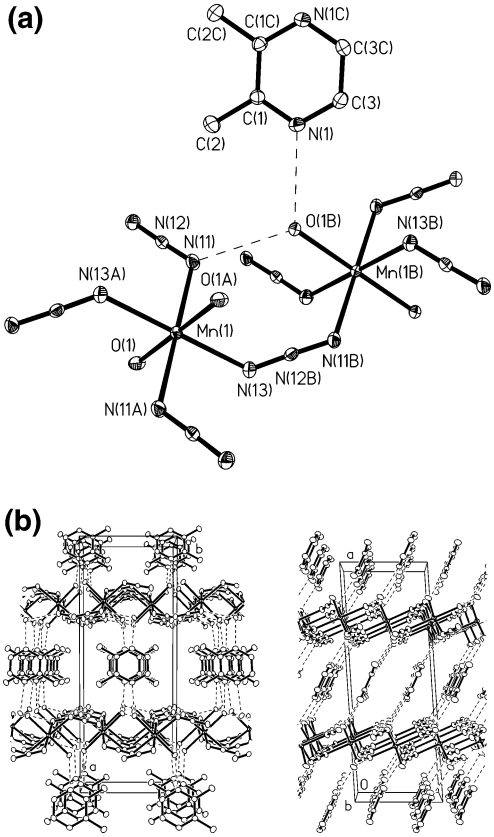

Figure 3. (a) ORTEP drawing of **3** showing the atom-numbering scheme. Ellipsoids are at the 50% probability level. Broken lines indicate hydrogen bonds. Symmetry codes are according Table 2. (b) Packing views of **3**.

N(12), and Mn(2)−N(23)−N(22C) are 134.70(11), 118.06(10), 124.93(11), and 130.34(11)°, respectively. The Mn(1)···Mn(2) intralayer distances are 5.534(2) and 5.676(2) Å, and the Mn−NNN−Mn′ torsion angles are 65.70(14) and 108.45(10)°, respectively. The acute angle between the Mn−N(azido) planes [defined by the Mn(1), N(11), N(21), N(11A), N(21A) and Mn(2), N(13), N(23), N(13B), N(23A) planes, respectively] is 79.30(5)°. Along the *c*-axis the Mn−azido layers are separated by the sheets of stacking ethylpyrazine molecules which act as monodentate ligands via their N(1) donor atoms. A supramolecular 3-D network structure is formed by hydrogen bonds of type O−H···N between O(1) of the aqua ligand and uncoordinated N(2) atoms of pyrazine ligands from adjacent layers [O(1)···N(2)(pyz) = 2.813(2) Å]. The intralayer hydrogen bond distance between O(1) and N(21) is 2.858(4) Å. The shortest interlayer Mn···Mn separation is 9.442(3) Å.

Only MnN_4O_2 chromophores are observed in the structure of **3** (Figure 3a,b; Table 2). Each manganese atom is bonded to four azido ligands and two axial water molecules. As in **1** and **2**, the metal centers are connected only by four EE bridging azides to generate the square Mn−azido layers. The 2,3-DiMepyz ligands remain uncoordinated. The Mn−N(azido) bond lengths are Mn(1)−N(11) 2.239(2) Å and Mn(1)−N(13A) 2.250(2) Å, whereas Mn(1)−O(1) is 2.1444(12) Å. The Mn−N−N bond angles Mn(1)−N(11)−N(12) and Mn(1)−N(13)−N(12B) are 122.53(11) and 129.02(11)°, respectively. The Mn−NNN−Mn torsion angle is −63.31(14)°, and the acute angle between two adjacent MnN_4(azido) planes is 85.47(5)°. The Mn(1)−Mn(1B) distance is 5.363(2) Å. Again a supramolecular 3-D network structure is formed by hydrogen bonds of type O−H···N between O(1) of the aqua ligand and uncoordinated N(1) atoms of pyrazine ligands from adjacent layers [O(1)···N(1)(pyz) = 2.791(2) Å], Figure 3b. Also there exist intralayer hydrogen bonds of type O−H···N between O(1) of the aqua ligand and the coordinated N(11) atoms of azido bridging ligands. The intralayer hydrogen bond distance between O(1B) and N(11) is 2.848(2) Å. The shortest interlayer Mn···Mn separation is 10.922(3) Å.

Description of the Structures of $[Mn(N_3)_2(Clpyz)_2]_n$ (4) and $[Mn(N_3)_2(Ipyz)_2]_n$ (5). The isostructural complexes **4** and **5** crystallize in the orthorhombic space group *Pbca*. Figures 4 and 5 illustrate the principal structural features together with the atom-labeling schemes of complexes **4** and **5**, respectively. Selected bond distances and angles for both complexes are listed in Table 2. In both structures the manganese atom is located in a trans octahedral environment. Each manganese atom is bonded to four azido ligands and two axial pyrazine derivative molecules, which act as monodentate ligands. The four azido ligands behave differently: two azido groups act as end-on bridging ligands between two manganese atoms giving rise to centrosymmetric planar Mn_2N_2 units, and the other two azides are end-to-end bridging. Each dimeric $[Mn_2(\mu_{1,1}\text{-}N_3)_2]^{2+}$ fragment is linked to four neighboring equivalent units by means of four

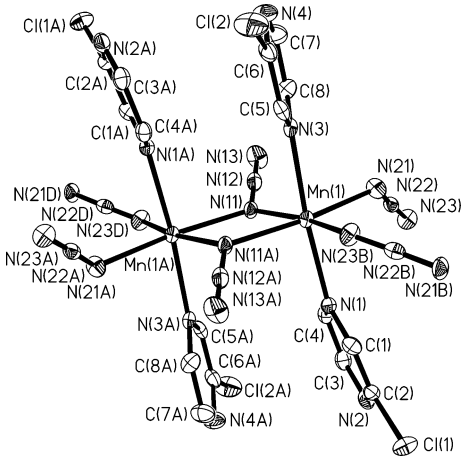

Figure 4. ORTEP drawing of **4** showing the atom-numbering scheme. Ellipsoids are at the 50% probability level. Symmetry codes are according Table 2.

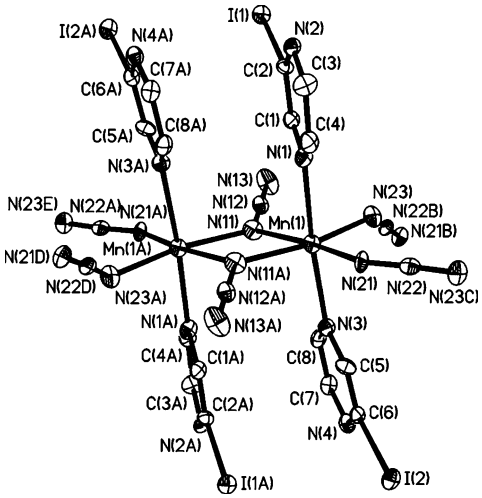

Figure 5. ORTEP drawing of **5** showing the atom-numbering scheme. Ellipsoids are at the 50% probability level. Symmetry codes are according Table 2.

single end-to-end azido bridges. Repetition of this basic scheme affords a neutral two-dimensional layer with a topology given in Chart 1, **1c**. In the case of **4**, the four-membered Mn_2N_2 units have a Mn(1)−N(11)−Mn(1A) bond angle of 100.9(2)° and a Mn(1)···Mn(1A) distance of 3.4214(14) Å. The single end-to-end azido bridge shows the Mn(1)−N(21)−N(22) and the Mn(1)−N(23B)−N(22B) bond angles of 128.0(3) and 145.0(4)°, respectively; the Mn(1)−N(23B)···N(21B)−Mn(1B) torsion angle is 58.8(5)°, and the Mn(1)···Mn(1B) distance is 5.772(2) Å. The angle between planes of neighboring Mn_2N_2 rings is 24.57(15)°. The shortest interlayer Mn···Mn distance is 12.448(3) Å.

In case of **5**, the four-membered Mn_2N_2 units have a Mn(1)−N(11)−Mn(1A) bond angle of 102.8(3)° and a Mn(1)···Mn(1A) distance of 3.4767(18) Å. The single azido bridge shows the Mn(1)−N(21)−N(22) and the Mn(1)−N(23)−N(22B) bond angles of 143.9(5) and 136.8(5)°, respectively, the Mn(1)−N(23)···N(21B)−Mn(1B) torsion angle is 30.1(6)°, and there is a larger Mn(1)···Mn(1B) distance of 5.845(2) Å. The angle between planes of neighboring Mn_2N_2 rings is 36.6(3)°. The shortest interlayer Mn···Mn distance is 13.635(4) Å.

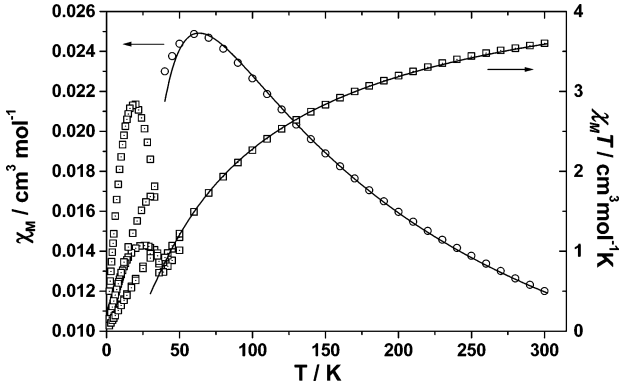

Figure 6. Plot of $\chi_M T$ (dot squares) and χ_M (open circles) vs T in the 300−2 K range of temperatures for $[Mn(N_3)_2(2,6\text{-DiMepyz})(H_2O)]_n$ (**1**) measured on cooling under external magnetic fields of 10000, 700, and 50 G (from top to the bottom in the plot) and plot of χ_M (open circles) vs T in the paramagnetic region of temperatures for **1.** The solid line shows the best fit in the paramagnetic region as a quadratic-layer Heisenberg antiferromagnet (see text).

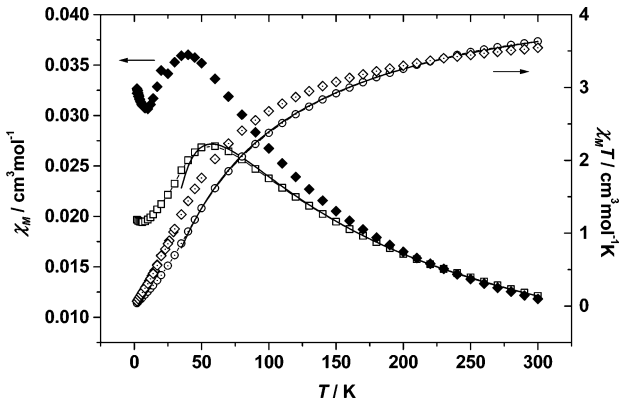

Figure 7. Plots of $\chi_M T$ (dot circles) and χ_M (open squares) vs T in the 300−2 K range of temperatures for $[Mn(N_3)_2(Etpyz)(H_2O)]_n$ (**2**) The solid line shows the best fit in the paramagnetic region as a quadratic-layer Heisenberg antiferromagnet (see text). Also shown are plots of $\chi_M T$ (dot squares) and χ_M (black squares) vs T in the 300−2 K range of temperatures for $[Mn(N_3)_2(Clpyz)_2]_n$ (**4**).

From the structural point of view, it should outlined that the use of the pyrazine derivatives 2,6-DiMepyz, Etpyz, 2,3-DiMepyz, Clpyz, and Ipyz (pyz = pyrazine (1,4-diazine)) in the reaction with Mn(II) and azido ligands allows in all the cases the syntheses of 2D compounds with only azido bridging ligands and two different topologies, **1a**,**c** from Chart 1. Moreover, the reaction among Mn(II), azido ligand, and pyrazine affords a 2D layered structure consisting in $\{Mn(\mu_{1,1}\text{-}N_3)_2\}_n$ chains bridged by the pyrazine ligand.[17]

Magnetic Data. The $\chi_M T$ products in the range 300−2 K for compounds **1**−**5** are plotted in Figures 6−9. **1**, **3**, and **5** show similar molecule-based magnet behavior: the $\chi_M T$ plots show a regular decay from room-temperature values of 3.60 $cm^3 \cdot K \cdot mol^{-1}$ for **1**, 4.03 $cm^3 \cdot K \cdot mol^{-1}$ for **3**, and 4.19 $cm^3 \cdot K \cdot mol^{-1}$ for **5** down to 35, 29, and 22 K critical temperatures, respectively, reflecting an overall antiferromagnetic behavior. Below the critical temperatures, $\chi_M T$ becomes field dependent. Under an external field of 40 G, the $\chi_M T$ value abruptly reaches the maximum value of 3.41 $cm^3 \cdot K \cdot mol^{-1}$ at 20 K for **1,** at an applied field of 50 G, the $\chi_M T$ value abruptly reaches the maximum value of 2.33 $cm^3 \cdot K \cdot mol^{-1}$ at 22 K for **3**, and under an external field of

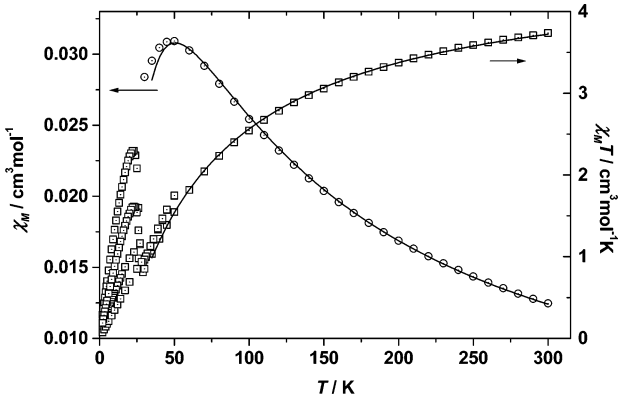

Figure 8. Plot of $\chi_M T$ (dot squares) vs T in the 300−2 K range of temperatures for $[Mn(N_3)_2(H_2O)_2]_n$(2,3-DiMepyz)$_n$ (**3**) measured on cooling under external magnetic fields of 4000, 200, 100, and 50 G (from top to the bottom in the plot) and plot of χ_M (dot circles) vs T in the paramagnetic region of temperatures for **3.** The solid line shows the best fit in the paramagnetic region as a quadratic-layer Heisenberg antiferromagnet (see text).

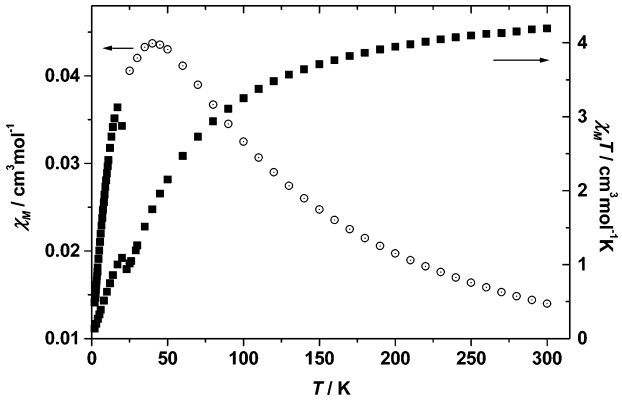

Figure 9. Plot of $\chi_M T$ (black squares) vs T in the 300−2 K range of temperatures for $[Mn(N_3)_2(Ipyz)_2]_n$ (**5**) measured on cooling under external magnetic fields of 3000 and 200 G (from top to the bottom in the plot) and plot of χ_M (dot circles) vs T in the paramagnetic region of temperatures for **5**.

200 G, the $\chi_M T$ value abruptly reaches the maximum value of 3.12 $cm^3 \cdot K \cdot mol^{-1}$ at 17 K for **5**. The χ_M value increases when the temperature decreases from 300 K up to a maximum of susceptibility (0.025 $cm^3 \cdot mol^{-1}$) found at 60 K for **1**, at 60 K for **2** (0.027 $cm^3 \cdot mol^{-1}$), at 50 K for **3** (0.036 $cm^3 \cdot mol^{-1}$), at 40 K for **4** (0.036 $cm^3 \cdot mol^{-1}$), and at 40 K for **5** (0.044 $cm^3 \cdot mol^{-1}$) due to the dominant antiferromagnetic coupling. After the maximum, the susceptibility value slowly diminishes and below T_c reaches abruptly 0.30 (40 G), 0.14 (50 G), and 0.24 $cm^3 \cdot mol^{-1}$ (200 G) at 2 K for **1, 3**, and **5**, respectively. Magnetization measurements performed between ±5 T at 2 K for **1, 3**, and **5** show magnetic hysteresis cycle and spontaneous magnetization with coercitive fields of 2000, 2000, and 1500 G for **1**, **3**, and **5**, respectively, Figure 10 for compound **1**. The magnetization at 2 K vs applied field for **3** and **5** has been added to the Supporting Information.

For **2** and **4**, the $\chi_M T$ or χ_M values at low temperatures are not field dependent and the magnetization measurements performed between ±5 T at 2 K do not show magnetic hysteresis cycle.

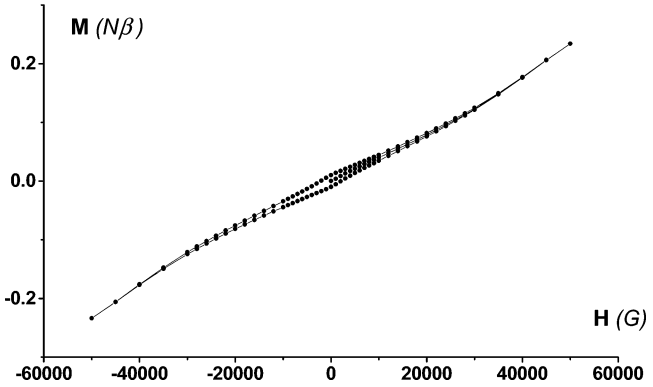

Figure 10. Magnetization at 2 K vs applied field for $[Mn(N_3)_2$(2,6-DiMepyz)$(H_2O)]_n$ (**1**). The solid line in the plot is a guide for the eye.

The compounds **1**−**3** show similar square-layer structures. The high-temperature susceptibility data for **1**−**3** in the range 300−50 K were fitted by the expansion series[53] of Lines for an $S = 5/2$ antiferromagnetic quadratic layer, on the basis of the exchange Hamiltonian $H = \Sigma_{nn} - JS_i \cdot S_j$, where Σ_{nn} runs over all pairs of nearest-neighbor spins i and j, eq 1, in which $\Theta = kT/|J|S(S+1)$. $C_1 = 4$, $C_2 = 1.448$, $C_3 = 0.228$, $C_4 = 0.262$, $C_5 = 0.119$, and $C_6 = 0.017$, and N, g, and μ_B have their usual meanings:

$$Ng^2\mu_B{}^2/\chi|J| = 3\Theta + (\Sigma C_n/\Theta^{n-1}) \qquad (1)$$

The best fit is given by the parameters $J = -4.9$ cm^{-1}, $g = 2.06$ for **1**, $J = -4.4$ cm^{-1}, $g = 2.05$ for **2**, and $J = -3.9$ cm^{-1}, $g = 2.05$ for **3**. This agrees with the superexchange values of $J = -4.2$, -4.2, and -3.5 cm^{-1} for **1**−**3**, respectively, expected from the position of the maximum given by the expression[53] (2):

$$kT_{max}/J = 1.12S(S+1) + 0.10 \qquad (2)$$

The analytical evaluation of the superexchange coupling constants is not possible for a manganese 2D system with one J ferro- and one J' antiferromagnetic parameter as in compounds **4** and **5**.

One open question is the reason for the existence of magnetic ordering and spontaneous magnetization for $T >$ 2 K in the compounds **1** and **3** but not in compound **2**, taking into account that **1**−**3** show the same square layers with only EE single azido bridges 2D structure in which the planes are connected by hydrogen bonds. In other published three Mn(II) compounds with the same structural 2D motif (see Table 3) it can be observed that only one of the three compounds shows magnetic ordering and spontaneous magnetization for $T >$ 2 K. This fact has been explained as a consequence of the J value and the angle between the mean Mn equatorial planes, which may induce a canting phenomenon.[4] The comparison of the mentioned compounds with **1**−**3** is difficult due to the reason that the former compounds show well-separated layers whereas the 2D layers in **1**−**3** are bridged by hydrogen bonds, as can be seen in the intersheet distances.

(53) Lines, M. E. *J. Phys. Solids* **1970**, *31*, 101.

Table 3. Comparison of Structural and Magnetic Data for the Two-Dimensional Manganese−EE Azido Systems (Chart 1, **1a**) Structurally Characterized to Date[a]

param	L = DENA	L = 4-acpy	L = Me-*i*-nic	**1**	**2**	**3**
Mn−N−N (deg)	148.4/171.7	129.0/151.6	128.3/149.7	127.7/124.2 123.6/132.2	134.7/118.1 124.9/130.3	122.5/129.0
Mn−N···N−Mn (deg)	180/166.7	100.4	96.8	−121.7/−59.1	65.7/108.4	−63.31
angle's mean planes (deg)	5.65	83.3	84.9	75.04	79.30	85.47
intersheet *d* (Å)	14.153	11.563	12.424	9.494	9.442	10.922
J (cm^{-1})	−3.42	−3.83	−2.24	−4.9	−4.4	−3.9
T_c (K)	<2	30	<2	35	<2	29
ref	4	2, 8	3	this work	this work	this work

[a] "Angle's mean planes" refers to the angle between the MnN_4 (N-azide) planes. Intersheet *d* is the minimum Mn−Mn interplane distance. T_c indicates the ordering temperature, if present. DENA = diethylnicotinamide, 4-acpy = 4-acetylpyridine, and Me-*i*-nic = methyl isonicotinate.

The second open question is the reason for the existence of magnetic ordering and spontaneous magnetization for $T > 2$ K in the compound **5** but not in compound **4**, taking into account that **4** and **5** are isostructural. One possible explanation is that, despite the isostructural character of **4** and **5**, the main bond angles related with the magnetic coupling are different: by example, the Mn−N···N−Mn torsion angles are 58.5(5) and 30.1(6)° for **4** and **5,** respectively, and the angles between planes of neighboring Mn_2N_2 rings are 24.57(15) and 36.6(3)° for **4** and **5**, respectively. Also, it should be taken into account that in **1, 3**, and **5** the low-temperature ordering corresponds to weak canting phenomena and small structural differences with similar compounds can affect largely the magnetic properties of the compounds at low temperatures.

Conclusion

Here we have presented five new 2D compounds with only azido as bridging ligand prepared from a new synthetic strategy: the reaction of manganese(II) nitrate with pyrazine derivatives and diluted hydrazoic acid in aqueous media. The new compounds are $[Mn(N_3)_2(2,6\text{-DiMepyz})(H_2O)]_n$ (**1**), $[Mn(N_3)_2(Etpyz)(H_2O)]_n$ (**2**), $[Mn(N_3)_2(H_2O)_2]_n(2,3\text{-DiMepyz})_n$ (**3**), $[Mn(N_3)_2(Clpyz)_2]_n$ (**4**), and $[Mn(N_3)_2(Ipyz)_2]_n$ (**5**) (pyz = pyrazine (1,4-diazine)). The 2D compounds **1**−**3** show the square layer topology **1a** (Chart 1) but with the novelty to incorporate water as axial ligand. In the case of **1** and **2** the water axial ligand alternates with the pyrazine derivative, but in the case of **3**, water is the only axial ligand and the 2,3-DiMepyz ligand, probably for steric hindrance, remains uncoordinated. The compounds **4** and **5** show **1c** topology (Chart 1) with pyrazine derivatives as axial ligands. **1, 3**, and **5** are molecule-based magnets showing magnetic ordering and spontaneous magnetizations below $T_c = 35$, 29, and 22 K, respectively. **2** and **4** do not show spontaneous magnetization up to 2 K.

Acknowledgment. This research was partially supported by the CICYT (Grant BQU2003-00538) and OENB (Grant 7967). F.A.M. thanks Prof. C. Kratky, Prof. F. Belaj (University Graz), and Prof. K. Gatterer and Dr. J. Baumgartner (TU-Graz) for use of experimental equipment.

Supporting Information Available: Tables of X-ray crystallographic data in CIF format for the structures reported in this paper and magnetization at 2 K vs applied field for $[Mn(N_3)_2(H_2O)_2]_n$-$(2,3\text{-DiMepyz})_n$ (**3**) and $[Mn(N_3)_2(Ipyz)_2]_n$ (**5**). This material is available free of charge via the Internet at http://pubs.acs.org.

IC051258Z